The STAR-TPC Slow Simulator

W.G. Gong (gong@lbl.gov)

February 26, 1995

1 Introduction

The response of a time-projection-chamber (TPC) can be simulated with respect to a charged cluster. By providing simulated data, a TPC simulator can serve the following purposes: (1) evaluate the TPC performance such as spatial resolution and two-track seperation; (2) optimize algorithms for cluster-finder and tracker; (3) test data compression for designing the Data Acquisition System; (4) function as an experimental filter for comparing model prediction with experimental data. Figure 1 represents a model for data processing. A fast simulator [1] has been used so far for physics simulations (level I). It is efficient, but lacks many physical considerations and an algorithm for cluster reconstruction. Implementation of a slow simulator together with a hit finder will provide an alternative but more realistic chain for physics simulations (level II). The realism of this simulator will be verified by actual data taken in future experiments (level III).

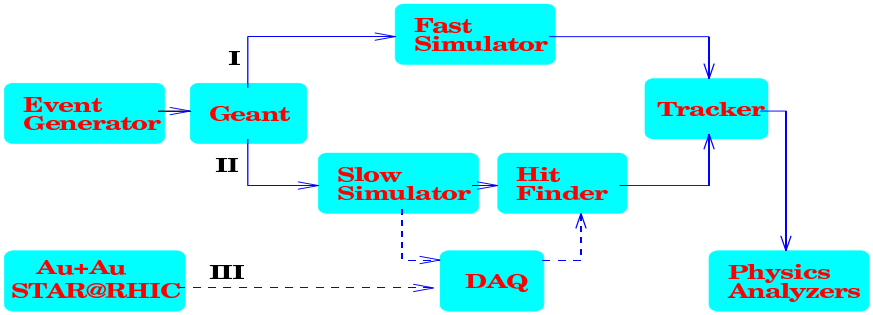

Figure 1: A data processing model

2 Model for the Slow Simulation

Figure 2 is a graphical model for the TPC slow simulator with the (x,y,z) coordinate system defined. An event generator produces particles in a nucleus-nucleus collision. Electron clusters along charged particle tracks are generated by the Geant in the TPC volume. Each cluster corresponds to a track segment of a few millimeters (in the direction perpendicular to anode wires). The number of electrons (n_e) is calculated by the ratio of energy loss (ΔE) over the average ionization potential (aip) of the gas mixture. This cluster of electrons is transported in a uniform electrical drift field from the space point to the sense wire plane. Both longitudinal and transverse diffusions are considered for the electron cloud. Gas gain fluctuation is incorporated according to the Polya function. After the avalanche, charges are spread over close-by pads in accordance with the measured pad response functions. The shaper response is folded with the longitudinally diffused cluster along the drift time. The signal amplitude is sampled at the SCA clock frequency. The shaper-filtered white noise is added to the signal at each time bucket for every pad affected. All the signals, pixel by pixel, are finally digitized to ADC counts once they are over a preset threshold level. Those ADC values with associated identifications of pad and time bucket are packed in a compact format as the simulated data.

In the following, we will give analytical expressions used in the STAR-TPC slow simulator. It is implemented in a package called *tss* in the STAR software library. This package was first prototyped by R. Morse [2], based upon subroutines provided by D. Roehrich and M. Levine [3]. But it was much improved and revised here. The

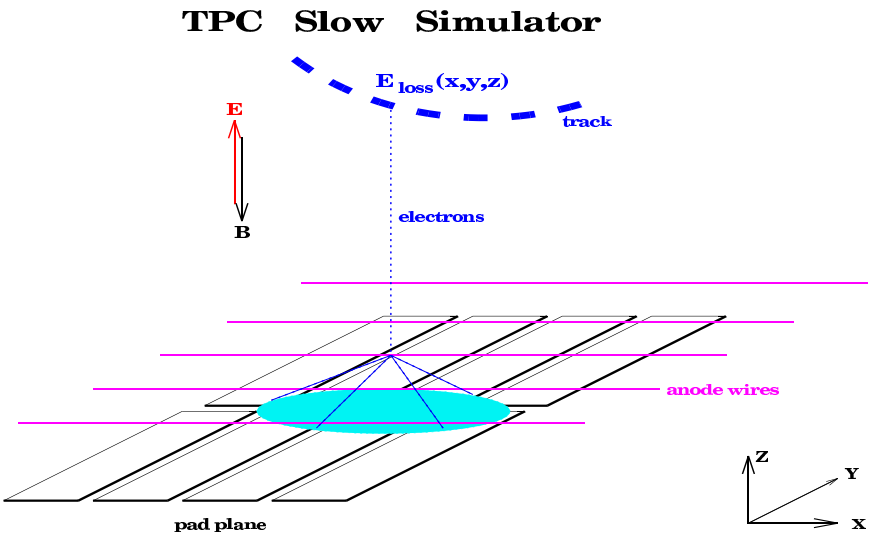

Figure 2: Schematic representation of a TPC slow simulator.

pad response function along a pad row was corrected, and the measured shaper response function was used. The pad response function across a pad row, avalanche gain fluctuation, and shaper-filtered white noise are all new features added in this work.

2.1 Pad Response

Assume a charged cluster originated from a space point at (x_0, y_0, z_0), the pad response along the anode wire (or along the pad row) is a convolution of the transverse diffusion function with the pad response function.

$$F(x_p, x_0) = \int_{-\infty}^{\infty} dx' \frac{\exp[-\frac{(x'-x_p)^2}{2\sigma_{prf}^2}]}{\sqrt{2\pi}\sigma_{prf}} \cdot \frac{\exp[-\frac{(x_0-x')^2}{2\sigma_t(z_0)^2}]}{\sqrt{2\pi}\sigma_t(z_0)} = \frac{\exp[-\frac{(x_0-x_p)^2}{2({\sigma_{prf}}^2+\sigma_t(z_0)^2)}]}{\sqrt{2\pi}\sqrt{{\sigma_{prf}}^2+\sigma_t(z_0)^2}} \tag{1}$$

where $\sigma_t(z_0) = \sigma_t\sqrt{z_0}$ and σ_t is the transverse diffusion constant.

For the pad response across the anode wire (or across the padrow), the pad response function is not a gaussian, but step functions defined by the wire positions. This function $f(y)$ is parameterized as:

$$f(y) = \varepsilon_1\Phi(y_1 - |y|) + \varepsilon_2[1 - \Phi(y_1 - |y|)]\Phi(y_2 - |y|) + \varepsilon_3[1 - \Phi(y_2 - |y|)]\Phi(y_3 - |y|) \tag{2}$$

where $\varepsilon_1 = 100\%$, $\varepsilon_2 = 50\%$, and $\varepsilon_3 = 5\%$. For the outer sector, $y_1 = 0.8cm$, $y_2 = 1.2cm$, and $y_3 = 1.6cm$. For the inner sector, $y_1 = 0.4cm$, $y_2 = 0.8cm$, and $y_3 = 1.2cm$. The convolution with the transversely diffused cluster gives

$$F(y_p, y_0) = \int_{-\infty}^{\infty} dy' f(y' - y_p) \frac{\exp[-\frac{(y_0-y')^2}{2\sigma_t(z_0)^2}]}{\sqrt{2\pi}\sigma_t(z_0)} \tag{3}$$

$$F(y_p, y_0) = \frac{1}{2}[(\varepsilon_1 - \varepsilon_2)\cdot\Delta erf(y_0, y_p, y_1) + (\varepsilon_2 - \varepsilon_3)\cdot\Delta erf(y_0, y_p, y_2) + \varepsilon_3\cdot\Delta erf(y_0, y_p, y_3)] \tag{4}$$

where $\Delta erf(y_0, y_p, y_i) \equiv erf(\frac{y_0-y_p+y_i}{\sqrt{2}\sigma_t(z_0)}) - erf(\frac{y_0-y_p-y_i}{\sqrt{2}\sigma_t(z_0)})$ for i=1,2,3, and $erf(y)$ is the error function. $\Phi(y) = 1$ (if $y \geq 0$), and 0 (if $y < 0$). (x_p, y_p) is the center of a pad.

We have measured the pad response for the STAR-TPC pads. As an example, Figure 3 shows convoluted pad responses measured for the inner sector pads (indicated by the points). The solid line in the right figure is the response function $f(y)$.

2.2 Shaper Response

Along the drift time direction, the response is a convolution of the shaper response function with a longitudinally diffused cluster. The shaper response function for one-stage differentiation and two-stage integration RC-CR

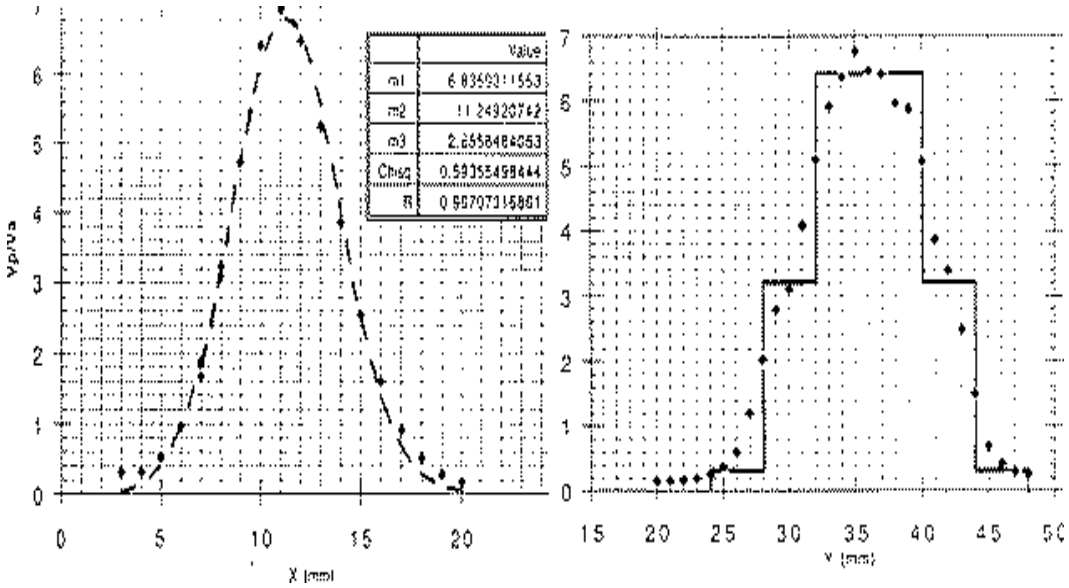

Figure 3: Measured pad response function for the inner-sector pad geometry: (a-left) response along a padrow (or anode wire); (b-right) response across a padrow (or anode wire).

shaper is

$$g(t,\tau) = \Phi(t)(\frac{t}{\tau})^2 \exp(-\frac{t}{\tau}), \tag{5}$$

which agrees well with the measured shaper response shown in Figure 4(a). The convoluted shaper response is then

$$F(t,t_z) = \int_{-\infty}^{\infty} dt' g(t-t',\tau) \frac{\exp[-\frac{(t'-t_z)^2}{2\sigma_l(z_0)^2}]}{\sqrt{2\pi}\sigma_l(z_0)} \tag{6}$$

$$F(t,t_z) = (\frac{\sigma_l(z_0)}{\tau})^2 \cdot \exp[\frac{\sigma_l(z_0)}{\tau}(\lambda - \frac{\sigma_l(z_0)}{2\tau})] \cdot [\frac{1+\lambda^2}{2}(1-erf(\frac{\lambda}{\sqrt{2}})) - \frac{\lambda}{\sqrt{2\pi}}\exp(-\frac{\lambda^2}{2})] \tag{7}$$

where $\lambda \equiv \frac{t_z - t}{\sigma_l(z_0)} + \frac{\sigma_l(z_0)}{\tau}$, $t_z \equiv \frac{z_0}{v_d}$, and v_d is the drift velocity.

2.3 Gain Fluctuation

Given an average gain G_0, the avalanche gain fluctuation follows the Polya distribution.

$$P(m) = \frac{m(mG/G_0)^{m-1}}{\Gamma(m)} \cdot \exp(-mG/G_0) \tag{8}$$

where m=1.5 typically for a multiwire proportional counter [4]. This distribution is sampled by the Monte-Carlo method between $G/G_0 = 0.1$ to 2.1 to generate the gas gain G (see Figure 4(b)).

2.4 Filtered White-noise

Since a shaper is usually band-width limited, white noises on the pad will become less "white" for the Switched-Capacitor-Array (SCA). To add noise to a pixel data, we use the shaper-filtered white-noise spectrum after renormalized to an Equivalent-Noise-Charge (ENC) value measured on the front end electronics. In the frequency domain, the power density for white noise is independent of frequency, but the phase for white-noise amplitude is undetermined. We choose the phase to be random [5]. The convolution of white-noise amplitude and the shaper response function in time domain can be computed with the help of Fast Fourier Transform (FFT).

$$N(t) = \frac{1}{\mathsf{N}}\mathsf{FFT}^{-1}[\exp(-i\phi) * \mathsf{FFT}g(t,\tau)] \tag{9}$$

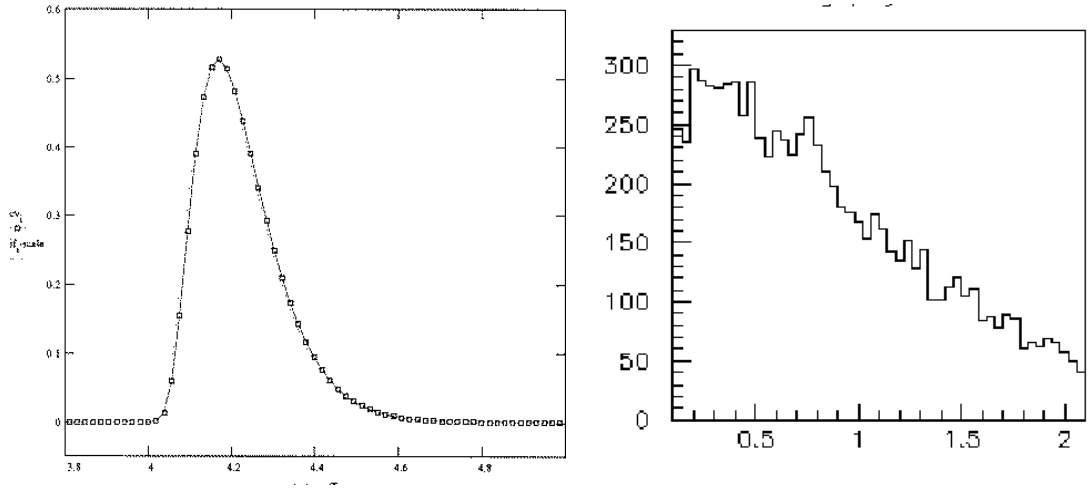

Figure 4: (a-left)Shaper response function (the x-axis is time in μsec); (b-right) Polya distribution for gain fluctuation (the x-axis is G/G_0).

where $\phi = 2\pi \cdot RNDM()$ is the random phase, and N is such a normalization constant that $N(t)$ will have a *rms* equal to the ENC value of the front end electronics.

2.5 Input Parameters

Putting everything together, we get the signal (in terms of electrons) for one pixel as follows:

$$S(x_p, y_p, t) = n_e \cdot G \cdot F(x_p, x_0) \cdot F(y_p, y_0) \cdot F(t, t_z) + N(t). \tag{10}$$

The following table lists input parameters used in the slow simulator.

tsspar table	Ar-CH_4 (10%)	He-C_2H_6 (50%)	unit/comment
ave-ion-pot (aip)	26.	41.	eV
gain-in (G_0^{in})	1000.	1000.	inner sector
gain-out (G_0^{out})	1000.	1000.	outer sector
v-drift (v_d)	5.5	2.5	cm/μsec
diff-const (σ_l)	0.0370	0.0170	cm/$\sqrt{cm}$
diff-trans (σ_t at B=0.5T)	0.0220	0.0220	cm/$\sqrt{cm}$
nsect	12	12	12×4 sectors
ntime	512	512	number of time bucket
tau (τ)	0.055	0.055	μsec
prf-in (σ_{prf}^{in})	0.25	0.25	cm
prf-out (σ_{prf}^{out})	0.40	0.40	cm
dynam	1023	1023	maximum of ADC
threshold	1.5	1.5	real ADC value
scale	670	670	No. el. per ADC
rms-noise (ENC)	800.	800.	electrons
geant-volm	0.4	0.4	cm

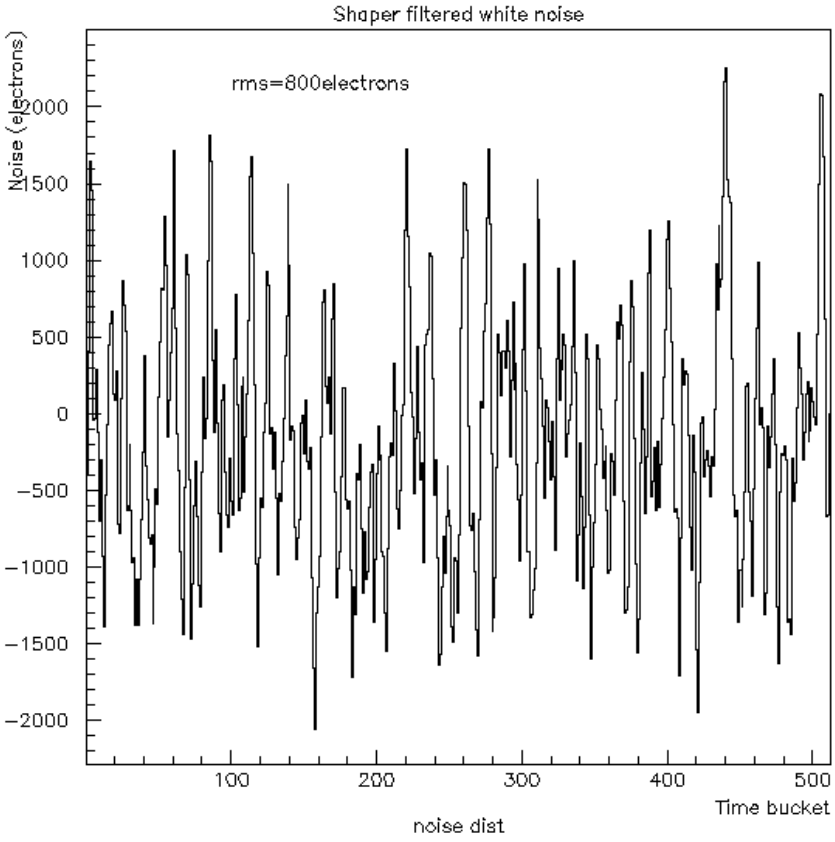

Figure 5: shaper-filtered white-noise spectrum (1 time bucket = 80 nsec).

3 Two-track Seperation

To study two-track seperation capability of the STAR-TPC, we generated three close tracks within each sector. They were pions of $P_t = 1.0GeV/c$, $\eta = 0.1(\theta = 84.3^o)$. The track seperations were set by $\Delta\theta = \Delta\phi = 0.5^o \cdot n$ where $n = 1, 2, ..., 6$. After running Geant to produce hits in the TPC volume, we ran the TPC Slow Simulator (*tss*) to generate pixel data. Figure 6 shows three dimensional plots of pulse height vs. pad number and time bucket on row #5 of the inner sector. Four sectors were choosen with $\Delta\theta = \Delta\phi$ ranging from 0.5^o to 2.0^o. Plots for other padrows at inner and outer sectors were similar. We find that $\Delta\theta = \Delta\phi \approx 1.0^o$ can be resolved by a hit-finder with simple deconvolusion algorithm. Two tracks at closer seperation may be possible to resolve with even better deconvolusion technique. This result is actually consistent with a simple estimate by $3 \times w_{pad}$ seperation between tracks when induced signal from each track spreads over 3 pad width (w_{pad}). For example, $\Delta\phi = \tan^{-1}(\frac{3\times 3.35mm}{600mm}) = 0.96^o$, for the first padrow of an inner sector, and $\Delta\phi = \tan^{-1}(\frac{3\times 6.67mm}{1271mm}) = 0.91^o$, for the first padrow of an outer sector.

4 One Event of Au+Au Collision

One HIJING event of Au+Au collision at E/A = 200 GeV/nucl. was used for our initial data analysis. A total of 705000 hits were generated by Geant. A total of 9 million pixel data were produced by the slow simulator (*tss*). This corresponded to an occupancy of 13% on average. Difficulty arose when this large volume of data was handled by Zebra. Fortunately, a new data format (XDF) has been implemented by C. Tull, W. Greiman, and D. Olson which can overcome this limitation. The new data format was proved to be necessary for processing one event of Au+Au collision in the TAS environment. Figure 7 displays a plot of pulse height spectrum vs. pad number and time bucket for the row # 44 in an outer sector. This kind of pixel data would then be processed later by another package for hit reconstruction.

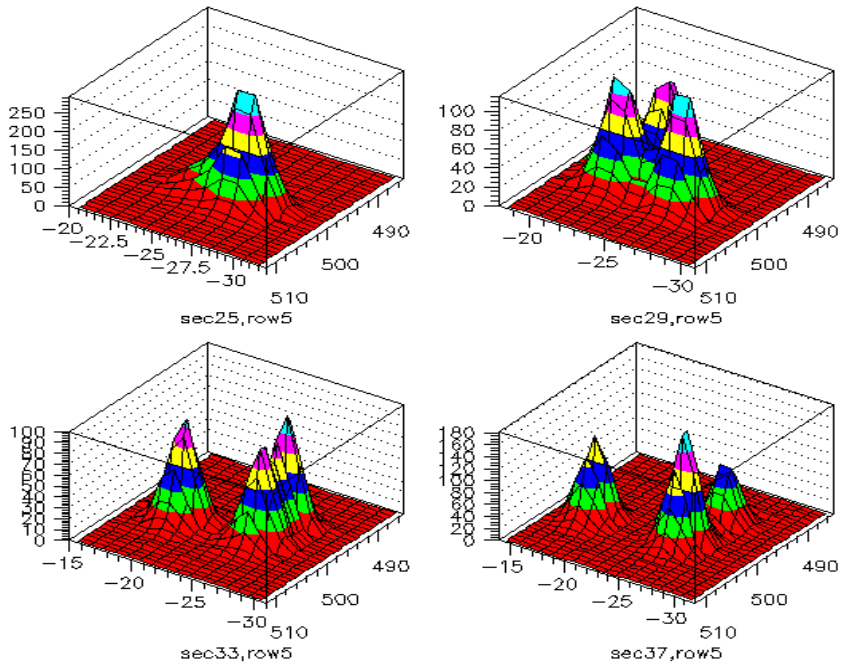

Figure 6: Two tracks at four different seperations: $\Delta\theta = \Delta\phi = 0.5^o$ (top-left), 1.0^o (top-right), 1.5^o (bottom-left), and 2.0^o (bottom-right).

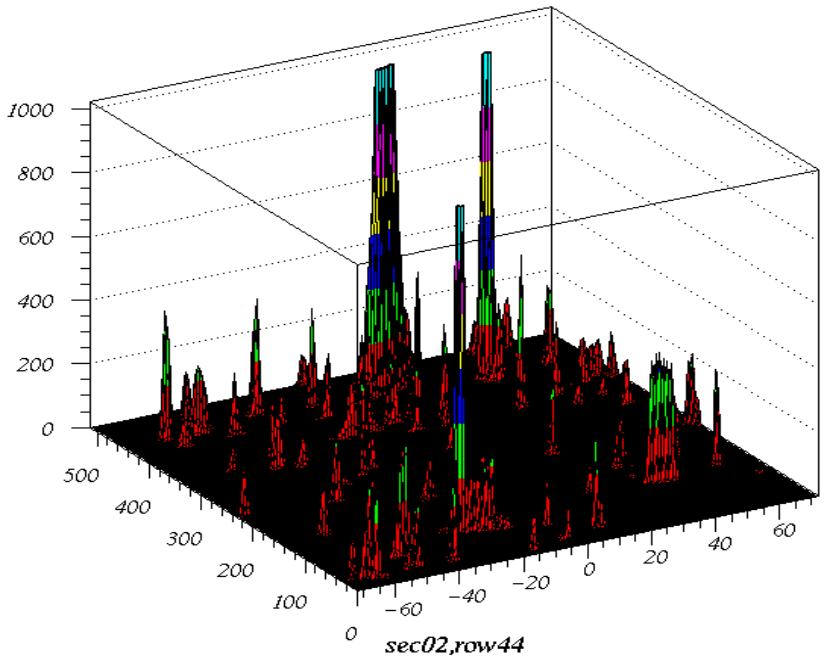

Figure 7: Pixel data output for a row#44 of sector #2 from one event of Au+Au collision.

5 Summary

We have implemented a slow simulator for the STAR-TPC. This version of slow simulator (tss) corrected treatments to pad response and to shaper response (found in the previous version). It added new features such as pad response across anode wires, gas gain fluctuation, and shaper-filtered white-noise. We have studied two-track seperation capability of the STAR-TPC which is around $\Delta\phi \approx \Delta\theta \approx 1.0^{o}$. We have processed one event of Au + Au collision at E/A = 200 GeV/nucl. and provided pixel data ready for hit-reconstruction. The averaged pixel occupancy was about 13%.

6 Acknowledgement

I would like to acknowledge helpful discussions with Howard Wieman on pad/shaper response functions and the filtered-white-noise, with Mike Lisa on debugging the previous version of slow simulator, with Iwona Sakrejda on running Geant. I should thank Doug Olson and Craig Tull for helping me out with TAS-related problems and for using the new data format (XDF).

7 References

1. P. Jones, I. Sakrejda, STAR-Note 0056.
2. R.J. Morse, LBL-35768, p140, 1994.
3. M.J. LeVine, D. Rohrich, proceedings of the STAR collaboration meeting (Jan. 1992)
4. R. Bellazzini and M.A. Spezziga, INFN PI/AE-94/02.
5. H. Wieman, private communication.